Effect of the nonspecific binding in differential impedance biosensing

Mathias Buff, Ewa Drab, and Kaori Sugihara

Citation: Biointerphases **14**, 011004 (2019); doi: 10.1116/1.5082717
View online: https://doi.org/10.1116/1.5082717
View Table of Contents: https://avs.scitation.org/toc/bip/14/1
Published by the American Vacuum Society

Effect of the nonspecific binding in differential impedance biosensing

Mathias Buff, Ewa Drab, and Kaori Sugihara[a)]
Department of Physical Chemistry, University of Geneva, Quai Ernest Ansermet 30, 1211 Geneva 4, Switzerland

(Received 23 November 2018; accepted 1 February 2019; published 11 February 2019)

The detection limits of impedance biosensors are dictated by the presence of background nonspecific binding, yet almost all the detection limits reported in the literature are determined using a clean buffer solution without confronting this real challenge. In this work, the authors employed the simplest "differential" impedance biosensor, composed of poly-L-lysine-polyethylene glycol-biotin-coated gold electrodes for the detection of streptavidin in the presence of 0.1% fetal calf serum, and studied the effect of the nonspecific binding on the performance of the differential impedance biosensing. The lowest streptavidin concentration detected by the system (5 μg/ml) was 1 order of magnitude higher (worse) than that from a previously demonstrated impedance biosensor where avidin was detected in the absence of background proteins. Interestingly, the origin of the differential signal was not due to the electrochemical properties of streptavidin itself but was that of the serum, where the coverage of the electrode by streptavidin indirectly modulated the electrical signal by suppressing the accessibility of the serum to the electrode. *Published by the AVS.* https://doi.org/10.1116/1.5082717

I. INTRODUCTION

Impedance biosensors detect the binding of analytes to an electrode surface coated with antibodies, DNA, oligonucleotide, and proteins by monitoring the change in the resistance or capacitance of the system in a label-free manner.[1] Compared to other label-free biosensors such as quartz crystal microbalance (QCM)[2] and surface plasmon resonance (SPR),[3] its instrumentation is notable for its low cost, low power, and ease of miniaturization. The literature reports its detection limit below 1 fg/ml,[4] which is several orders of magnitude lower than that of the current most successful point-of-care diagnostic device, lateral flow immunoassays,[5] without enhancement. Therefore, impedance biosensors may hold great promise for replacing lateral flow immunoassays as a point-of-care diagnostic tool with improved sensitivity. However, despite exhaustive efforts in recent decades, not even a single impedance immunoassay has yet made it to wide commercial success. This is because, although its sensitivity is high, its selectivity is extremely poor.

The selectivity of surface-based biosensors depends on the amplitude of the signal produced by the specific binding of analytes to the sensor surface in comparison to the nonspecific binding of background molecules.[6] To suppress the nonspecific binding, the sensor surface is often pre-exposed to a solution containing a blocking agent (e.g., bovine serum albumin) or antifouling agents [e.g., polyethylene glycol (PEG)].[7] Nonetheless, these blockings are never perfect; thus, the limit of detection in many practical situations is dictated by the presence of nonspecific binding. For example, the concentration of the tumor marker for hepatocellular carcinoma (liver cancer) in blood is in the order of ng/ml,[8] while that of serum albumin in blood is in the range of 50 mg/ml.[9] This highlights the great challenge we are facing in terms of selectivity. The effect of these background proteins is also called "macromolecular crowding" in cell biology, where it has been found to alter dramatically the properties of proteins, such as their effective concentrations, binding affinity to other molecules, and so on.[10] Almost all the detection limits reported in the literature have been determined under clean buffer solution without confronting this real challenge. For impedance biosensors targeting point-of-care diagnostic devices, the samples are body fluids from patients; therefore, the poor selectivity is one of the main bottlenecks, hindering its practical success.

To overcome this issue, Maupas, in 1997, introduced the concept of differential techniques in impedance biosensing.[11] The technique uses an additional "reference sensor" to measure the nonspecific binding separately. The reference sensor is composed of an electrode covered with fake antibodies or antifouling materials so that the analytes do not bind specifically. The signal from the analyte-antibody binding will be extracted as a difference between responses from the working and reference sensors. The use of the reference sensor then cancels out the effect of nonspecific adsorption, thus enabling an accurate detection of analytes in the presence of other background compounds. In their work, this technique was demonstrated briefly at a single analyte concentration of 0.5 mg/ml. The same concept has become the standard in SPR biosensing, resulting in moderate success.[12] However, in the case of impedance-based detection, little progress has been reported in the literature since publication of the original study;[13] therefore, the effect of the nonspecific binding on the differential measurements has not yet been studied fully.

In this work, to study the sensitivity of differential impedance biosensing in the presence of serum, we demonstrated the

[a)]Author to whom correspondence should be addressed: kaori.sugihara@unige.ch

simplest impedance biosensor, where gold electrodes are coated with poly-L-lysine (PLL)-PEG-biotin; the streptavidin in solution was detected in the presence of fetal calf serum (FCS).

II. MATERIALS AND METHODS

A. Ligands and solutions

The buffer solution was prepared with 10 mM 4-(2-hydroxyethyl)piperazine-1-ethanesulfonic acid (Fisher Scientific, USA) and 0.15M sodium chloride (Sigma Aldrich, Switzerland) in ultrapure water filtered through MilliQ Gradient A10 filters (Millipore AG, Switzerland). The *p*H was adjusted to 7.4 using 6M NaOH (Reactolab SA, Switzerland). It was sterile filtered through 0.22 μm porous membranes before use. For the demonstration of the differential technique, FCS (2-01F10-I, Bioconcept, Switzerland) and/or streptavidin (#S4762, Sigma Aldrich, Switzerland) was added at desired concentrations.

B. Surface functionalization of electrodes

10 nm titanium followed by a 50-nm gold layer was deposited via sputtering (Plassys MEB550S electron-beam evaporator, Paris, France) on silicon wafers (UniversityWafer, Boston MA, USA). They were cut to roughly 1.2 cm × 3.0 cm so that they fit the electrochemical chamber. PLL-g-PEG-biotin [Mw ≈ 22.7 kDa, #PLL(20)-g[3.5]-PEG(2)/PEG(3.4)-biotin(50%)] and PLL-g-PEG [Mw ≈ 22 kDa, #PLL(20)-g[3.5]-PEG(2)] were purchased from SuSoS AG (Switzerland). After cleaning the electrodes with acetone (Thommen, Switzerland), isopropanol (Fisher Scientific, Switzerland), and MilliQ water, they were activated using an oxygen-plasma cleaner (TePla IoN 3Mz oxygen plasma machine, PVA TePla, Germany) and incubated under PLL-g-PEG or PLL-g-PEG-biotin dissolved in HEPES buffer solution at 1 mg/ml for 24 h, followed by a rinse with MilliQ water and dried with a nitrogen stream.

C. Electrochemical impedance measurements

Electrochemical measurements were performed with an AUTOLAB PGSTAT302N-FRA32M potentiostat (Metrohm AG, Switzerland) and NOVA 2.1 as the monitoring software, with the three-electrode measurement setup, where stainless steel was used as a counter, Ag/AgCl as a reference, and the gold-deposited silicon wafer as a working electrode. The half-homemade electrochemical chamber was built on a cell purchased from Zensor R&D (#SF100, Taiwan ROC) and modified so that the electrical contact to the working electrode was enabled from the top (gold side) with an active electrode area of around 0.5 cm^2. In all impedance measurements, a sinusoidal AC voltage of 10 mV at open circuit potential was applied and the current response of the system was measured over time at a fixed frequency[14] ranging from 520 to 620 Hz. The solution flow was controlled with an NE-300 syringe pump (New Era Pump Systems, Inc.) and a Cheminert C22-6186 loop injector (Valco Instruments Co. Inc.). During the impedance measurements, the solution flow rate was fixed at 175 μl/min. Based on the flow speed and the volume of the electrochemical chamber, the incubation time of each solution was roughly estimated at 700 s. For the analysis of the impedance signals, we selected data points roughly 1200 s after the injection, and the baseline drift was subtracted.

D. Fluorescence microscopy

Fluorescent images were acquired using a Nikon Eclipse Ti-E inverted fluorescence microscope (Nikon AG, Switzerland) equipped with a CCD camera (DS-Qi2, Nikon), a TRITC filter cube (excitation 532–554 nm, emission 573–613 nm, and dichroic mirror 562 nm), and a 10× (Nikon CFI Plan Fluor DL 10XF) air objective. All fluorescent images were analyzed using IMAGEJ and presented with a false color. Samples for fluorescence microscopy were fabricated as follows: Electrodes functionalized by polymers were incubated with 1-μl droplets of fluorescent streptavidin solution at 1 mg/ml (#S11227, Streptavidin, Alexa Fluor™ 594 conjugate, ThermoFisher, Switzerland) for 15 min, then rinsed thoroughly with MilliQ water and dried with a nitrogen stream.

E. Quartz crystal microbalance with dissipation monitoring

Quartz crystal microbalance with dissipation monitoring was performed on Q-SENSE (Biolin Scientific, Sweden) by using Quartz Crystal 4.95 MHz, AT-cut coated with a 100-nm gold layer (QS-QSX301 Gold, Biolin Scientific, Sweden) as a sensor. The change in the adsorbed mass and the viscoelastic properties of the formed film were measured simultaneously in real time by monitoring the frequency Δf and dissipation ΔD, respectively. The working temperature was set to 25 °C. Prior to use, sensors were cleaned by immersing them in a mixture of 30% hydrogen peroxide, 25% ammonia, and MilliQ water at 75 °C for 5 min, followed by extensive rinsing with MilliQ water and drying under nitrogen flow. Crystals were treated with UV/ozone for 20 min, incubated with PLL-g-PEG-biotin [Mw ≈ 22.7 kDa, #PLL(20)-g[3.5]-PEG(2)/PEG(3.4)-biotin(50%)] or PLL-g-PEG [Mw ≈ 22 kDa, #PLL(20)-g[3.5]-PEG(2)] solutions for 24 h and rinsed with buffer solution (10 mM HEPES, 150 mM NaCl).

III. RESULTS AND DISCUSSION

To study the effect of nonspecific binding on the differential impedance biosensing technique, we demonstrated the simplest biosensor based on gold electrodes coated with PLL-g-PEG-biotin for the detection of streptavidin [Fig. 1(a)]. The reference sensor was composed of gold electrodes coated with PLL-g-PEG, where PEG is often used as a passivation layer.[15] Streptavidin does not specifically adsorb on PLL-g-PEG; therefore, this reference sensor measures only the nonspecific binding. Impedance detection of avidin with biotin-coated electrodes has previously been reported, which yielded the limit of detection in a nanomolar range (≈100 ng/ml) under clean buffer solution,[16] where the impedance spectroscopy was used instead of overtime

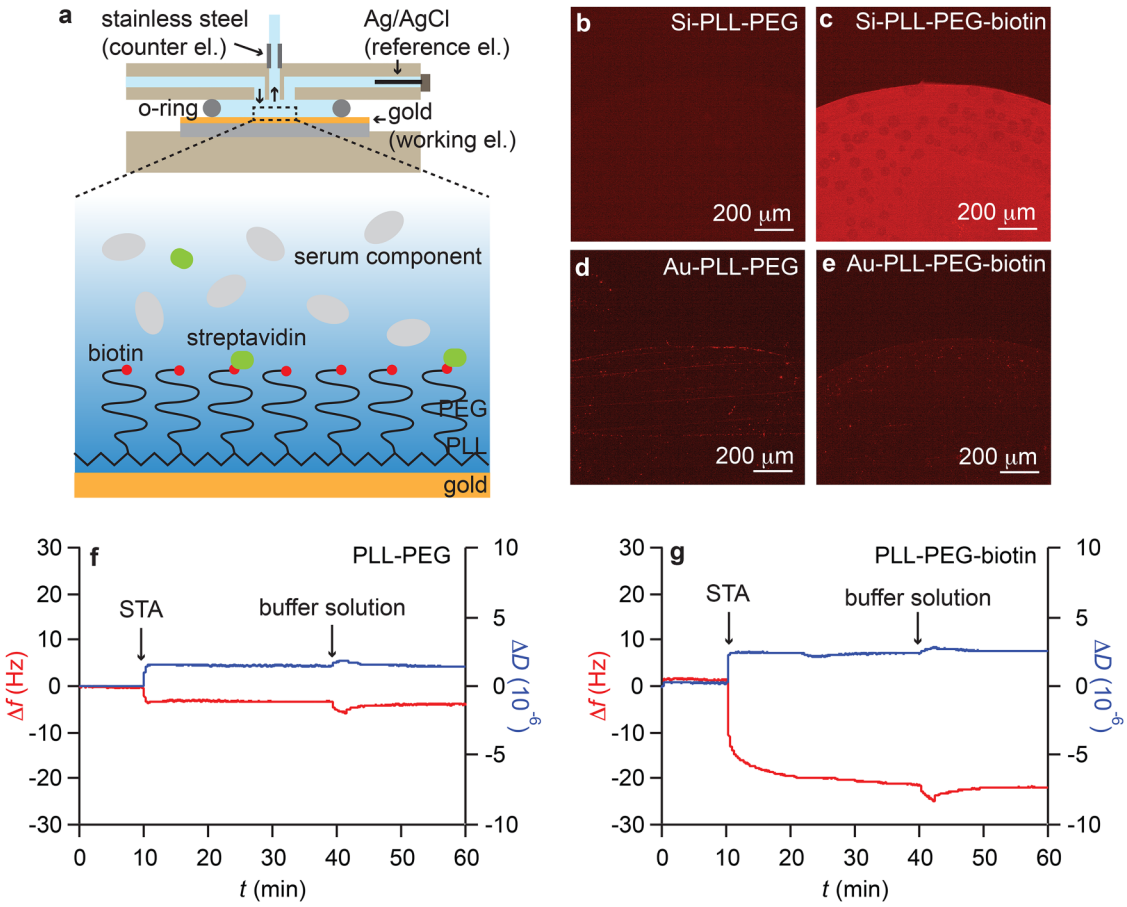

FIG. 1. (a) Scheme showing the concept of the biosensing. Fluorescence images of Alexa Fluor 594-labeled streptavidin, incubated on [(b) and (d)] PLL-g-PEG and [(c) and (e)] PLL-g-PEG-biotin-functionalized silicon and gold electrodes, respectively. (f) and (g) QCM-D data during the injection of streptavidin at 25 μg/ml with PLL-PEG and PLL-PEG-biotin coated gold QCM crystals, respectively.

monitoring at fixed frequencies. The specific adsorption of streptavidin on PLL-g-PEG-biotin was confirmed by fluorescence microscopy by monitoring the attachment of fluorescently labeled streptavidin [Figs. 1(b)–1(e)]. This approach visualized the fluorescence intensity contrast between PLL-PEG (nonspecific adsorption) and PLL-PEG-biotin (specific adsorption) on silicon wafers [Figs. 1(b) and 1(c)], yet it was much less on gold electrodes, because gold quenches the fluorescent dyes [Figs. 1(d) and 1(e)]. To ensure the functionalization of the gold substrates, a quartz crystal microbalance with dissipation monitoring (QCM-D) was used to detect the binding of the streptavidin. The injection of streptavidin at 25 μg/ml induced a large frequency shift for the PLL-PEG-biotin-coated gold QCM crystal [Fig. 1(g)], but a much smaller shift for the one with PLL-PEG [Fig. 1(f)], confirming the successful coating of gold with these polyelectrolytes. Even for the gold crystal coated with PLL-PEG, a slight streptavidin adsorption (nonspecific binding) was observed.

For the demonstration of impedance biosensing, we monitored the current over time while applying 10 mV AC voltage at a fixed frequency at the open circuit potential ($V_{\text{offset}} = V_{\text{OCP}}$) during the injection of analytes. Often, impedance biosensing is performed by measuring the impedance spectroscopy at zero offset potential $V_{\text{offset}} = 0$, where the impedance spectra are obtained before and after the injection of analytes into the electrochemical chamber.[17] However, such measurements inherit errors in their signals, because each time the program starts to take the impedance spectrum, the potentiostat applies a voltage up to 300 mV to counterbalance the open circuit potential of the system for establishing $V_{\text{offset}} = 0$. Then, as the program finishes, the system tries to recover the open circuit potential; both of these actions induce a large capacitive current that rearranges the ion configurations on the electrodes and dramatically alters the electrical signals (see Figs. S1 and S2 in the supplementary material[18]). Often, impedance measuring is described as a noninvasive technique, due to the applied small (10 mV) AC voltages. Nevertheless, one should not forget that this counter-voltage applied by the instrument to establish $V_{\text{offset}} = 0$ is 1 order of magnitude larger than the amplitude of the AC voltage. There is an informative previous report that suggests this issue and proposes impedance measurements at open-circuit potential.[16] Inspired by this work, we performed all the experiments at the open circuit potential and as continuous overtime measurements at fixed frequencies, which enabled us to avoid switching the offset voltage on and off. In addition, we controlled the solution flow with a syringe

pump and a loop injector, to avoid the fluctuation of the signals due to the injection pressure [Fig. S1 (Ref. 18)]. These two points, maintaining a constant offset voltage and controlling the fluid flow, are sometimes overlooked in the impedance biosensing, yet they are critically important for yielding accurate and reproducible measurements. In addition, to avoid a low frequency (<100 Hz) that contains a larger baseline drift, to keep all the used solutions in use at room temperature, to degas all of the solutions beforehand to minimize the presence of air bubbles in the chamber, and to use identical wire connections for all the measurements helped us to stabilize the baseline. Waiting a long time after the injection of the first buffer solution further reduced the baseline drift. The criterion for the baseline to be able to perform impedance sensing is that the baseline drift must be at least at the same order of magnitude as the signal. Therefore, so long as this criterion was fulfilled, we waited only about 10 min to stabilize the baseline, so as not to sacrifice the throughput of the experiments.

The differential measurements were performed by monitoring four parameters: $|Z|$ (absolute impedance value), Z' (real component), $-Z''$ (imaginary component), and phase over time, while injecting solution (streptavidin, STA, at 0.5–50 μg/ml mixed in HEPES buffer solution with 0.1% FCS) into the electrochemical chamber. The working sensor was coated with PLL-PEG-biotin, and the reference sensor with PLL-PEG. Here, we present $-Z''$ (imaginary component) and phase data, while $|Z|$ (absolute impedance) and Z' (real component) are shown in Figs. S3 and S4, respectively, in the supplementary material (Ref. 18). Previous reports have suggested that a too-high frequency (above 10 kHz) contains only the information of the bulk solution [the data in our case are shown in Fig. S5 (Ref. 18)], while a too-low frequency (below 100 Hz) has a large amount of noise and suffers from the intense signal drift over time, due to the large absolute values in the parameters; thus, an intermediate frequency in the range of around 1000 Hz is usually selected.[11] In addition, the instability reported by Maupas

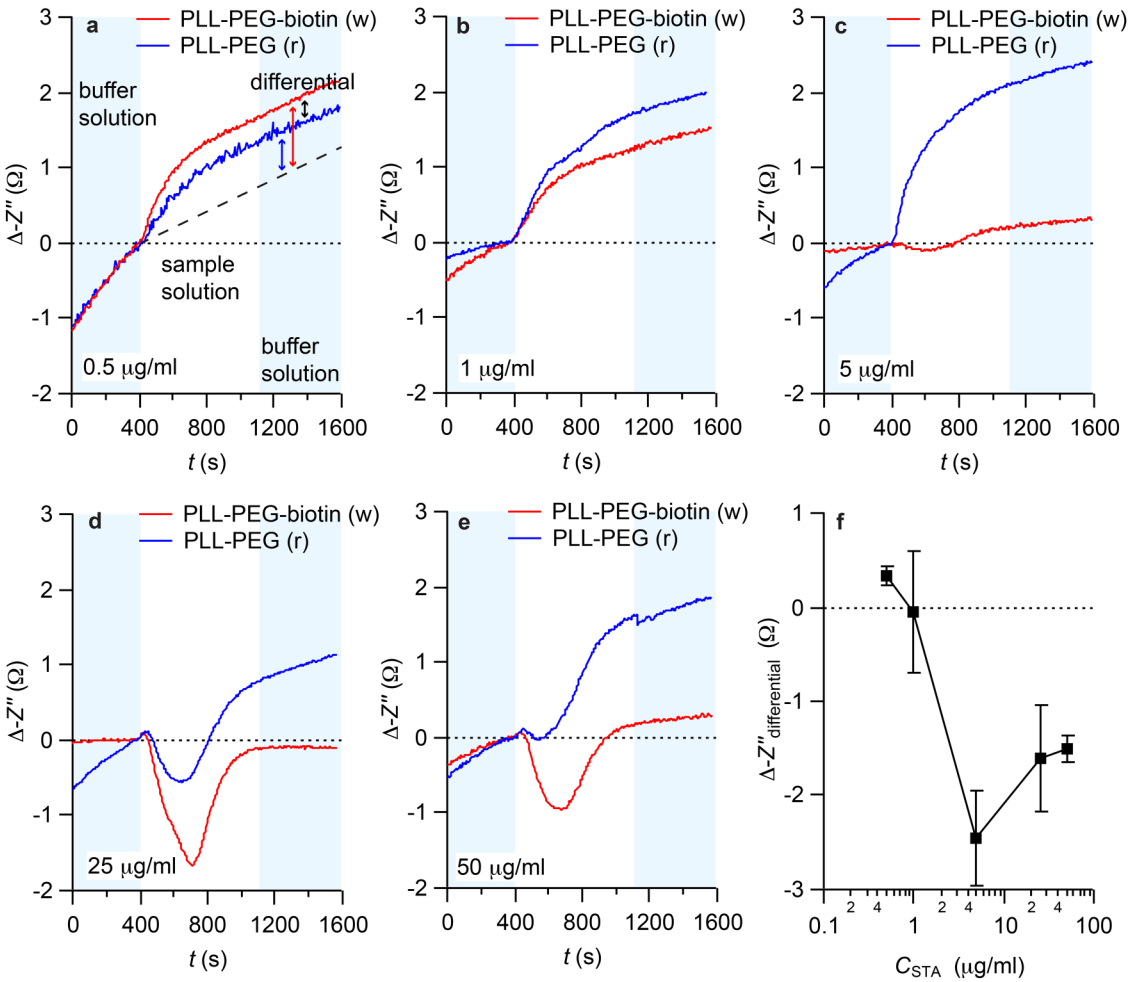

FIG. 2. Variation in Δ-Z'' during the differential measurements at (a) 0.5, (b) 1, (c) 5, (d) 25, and (e) 50 μg/ml streptavidin (STA) concentrations. The concentration of FCS was kept at 0.1% for all the samples. Measurements at each concentration were performed with working (PLL-PEG-biotin, red) and reference (PLL-PEG, blue) sensors. The timing of the sample injection and rinse is indicated with light blue and white background colors. Note that the solution exchange takes place gradually due to the relatively slow flow rate and the volume of the chamber (see Sec. II). (f) The differential signal $(\Delta\text{-}Z''_{\text{working}}) - (\Delta\text{-}Z''_{\text{reference}})$ was plotted against STA concentrations. Each concentration was repeated at least for a few times for obtaining the standard deviations as error bars.

et al.[11] was also observed in our system below ~300 Hz. Therefore, in our experiments, we fixed the frequency at $f = 520$–620 Hz to avoid the complications that come below 300 Hz, yet ensuring a frequency low enough for detecting the response from the electrode-solution interface. Note that we used a loop injector; thus, the injection of the sample solution was automatically followed by a rinse with HEPES buffer solution after roughly 700 s. All the measurements were performed at open circuit potentials ($V_{OCP} \approx 290$ mV). The working and reference sensing were performed separately. Measurements were conducted at each concentration with a new electrode, to avoid the saturation, unless otherwise mentioned, and repeated at least a few times, to study the reproducibility.

First, for the reference sensors (PLL-PEG), when STA solution at 0.5 μg/ml (in HEPES buffer solution at 0.1% FCS) was injected after the baseline was stabilized with HEPES buffer solution, a positive signal was observed in $-Z''$ [blue in Fig. 2(a)], indicating that a nonspecific binding was detected. When the same solution was injected into the working sensors (PLL-PEG-biotin), a positive signal was also observed [red in Fig. 2(a)]; this includes the response from both the specific and nonspecific bindings. Therefore, in differential measurements, their difference (≈0.4 Ω) was interpreted as the signal from the specific binding (only if it was significant compared to the errors). When STA solution at higher concentrations (1–50 μg/ml) was injected [Figs. 2(b)–2(e)], these differential signals varied [Fig. 2(f)]. Note that, in this work, we analyzed the subtraction values between the working and the reference signals for the sake of simplicity, as was done in the original work by Maupas *et al.*[11(a)] The fraction of the binding sites occupied by the ligands has previously been linked to another function of admittance.[13(a)] The reproducibility of the measurements was not very good, as evidenced by the relatively large error bars [Fig. 2(f)]. Typically, impedance biosensing under clean buffer solution is performed by the sequential injection of a solution with ligands onto an identical electrode, and the response is plotted against the ligand concentration to present the dose curve.[4] Such an experiment could yield small errors if the signal does not saturate, yet it does not represent the sensor's performance in a realistic situation

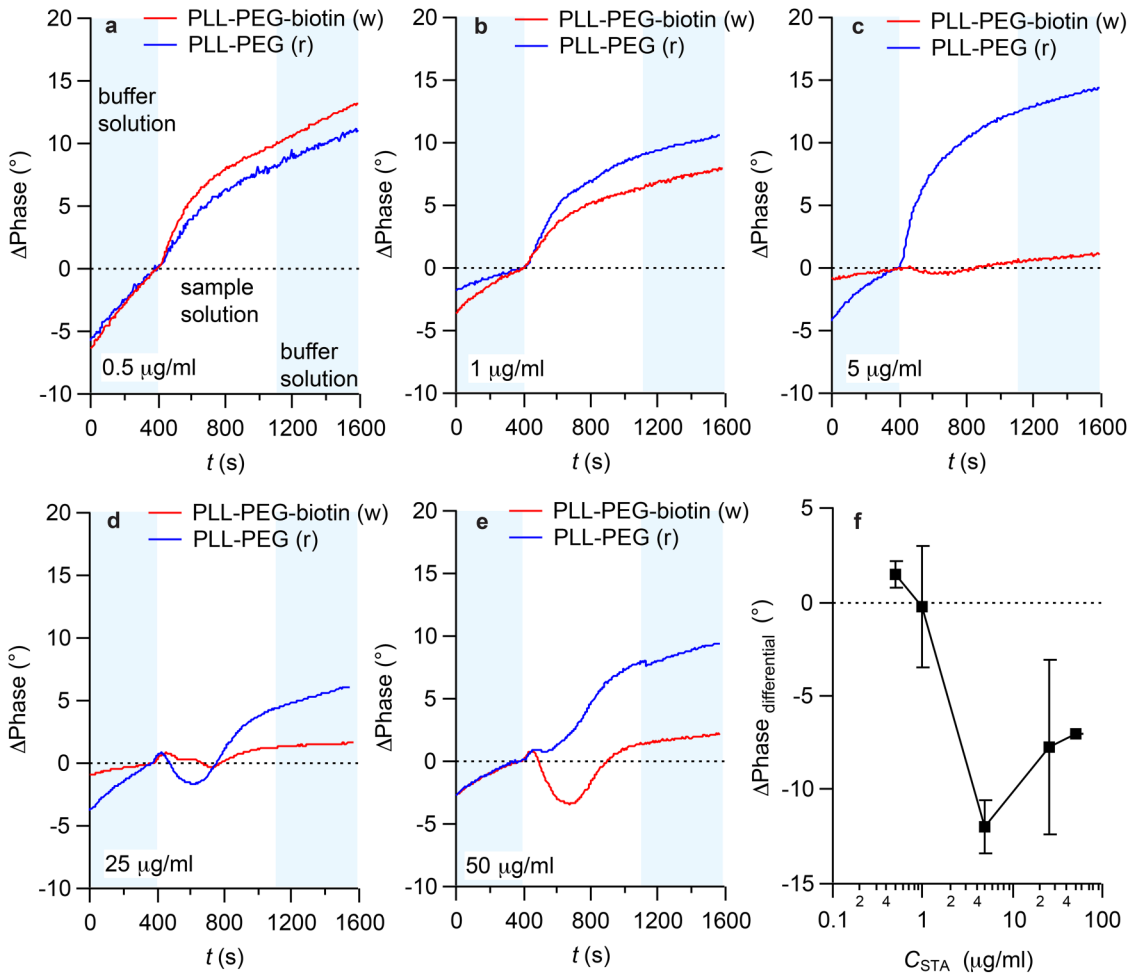

FIG. 3. Variation in phase during the differential measurements at (a) 0.5, (b) 1, (c) 5, (d) 25, and (e) 50 μg/ml streptavidin (STA) concentrations. The concentration of FCS was kept at 0.1% for all the measurements. Measurements at each concentration were performed with working (PLL-PEG-biotin, red) and reference (PLL-PEG, blue) sensors. (f) The differential signal $(\Delta\text{Phase}_{working}) - (\Delta\text{Phase}_{reference})$ was plotted against STA concentrations.

where new electrodes are used in each measurement. The poor reproducibility shown in this work [Fig. 2(f)] highlights another challenge in impedance biosensing that is also often neglected. Nevertheless, the differential signal changes between lower STA concentrations (0.5–1 μg/ml) and the higher ones (5–50 μg/ml). Considering the error bars that result from a few experiments with each concentration, we were disappointed to be able to detect the presence of STA only at 5 μg/ml or higher; further, the differential signals do not tell the exact concentration of STA, because the response immediately saturates at concentrations higher than 5 μg/ml. A similar trend was also observed in phase (Fig. 3), yet, due to the large error bars, it was not suitable for sensing in this system. The saturation of the impedance signals has previously been interpreted as the complete coverage of the binding sites.[13(a)] The lowest STA concentration detected in the presence of 0.1% FCS in this work (5 μg/ml) is 1 order of magnitude higher (worse) than that from the previous avidin impedance-based biosensor in the absence of background proteins (≈100 ng/ml)[16] and 9 orders of magnitude higher than the best performance of impedance biosensing reported in the literature (fg/ml).[4] This result highlights how the presence of background molecules changes the sensitivity of an impedance biosensor by orders of magnitude.

To interpret our differential signals in greater detail, we performed control experiments, where STA and FCS were detected separately under clean buffer solution. For the FCS solution, we observed a positive response both in $-Z''$ and phase, which is consistent with the differential measurements [Figs. 4(a) and 4(b)]. In this experiment, the FCS solution was injected sequentially. Therefore, the effect of saturation was observed at 10% FCS, where the signal from FCS adsorption starts to become smaller. Counter-intuitively, much smaller signals were observed when STA was injected in the absence of FCS [Figs. 4(c) and 4(d)], compared to those in the presence of FCS (Figs. 2 and 3). The sensitivity of the impedance signal depends on how the attachment of the analyte changes the electrical components in the system, such as charge transfer resistance R_{ch} and double layer capacitance C_{dl}. For example, when the analyte is relatively permeable to ions or if they are not tightly packed on the electrode, their presence affects neither the charge transfer resistance R_{ch} nor the double layer capacitance C_{dl} in a significant way. Therefore, it is not surprising that some molecules cannot be detected very well using impedance measurements like streptavidin, in our case. Note that the sensitivity against streptavidin alone is not zero, as the zoom-in plot [inset in Fig. 4(c)] shows a slight signal change upon the injection of streptavidin. These control experiments [also see Fig. S6 (Ref. 18)] suggest that both of our electrodes primarily detected only FCS and had extremely poor sensitivity toward STA.

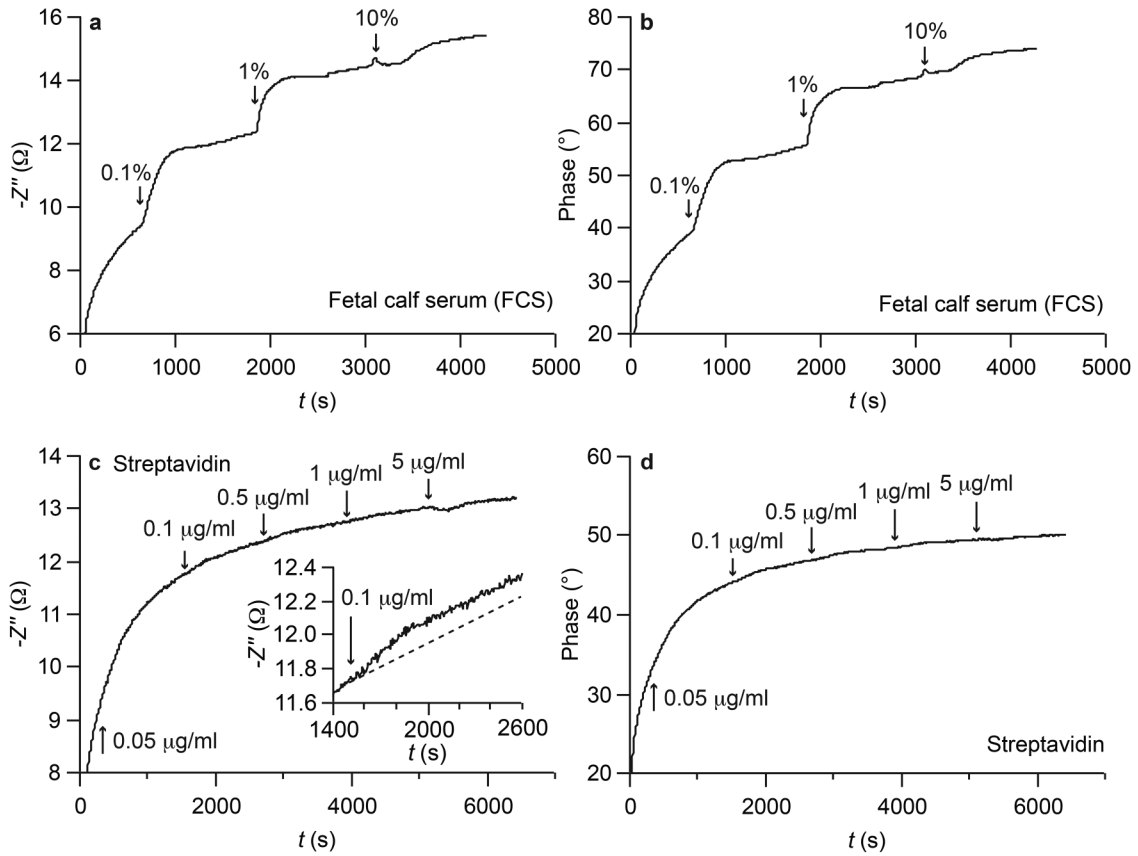

FIG. 4. Control experiments, where [(a) and (b)] FCS and [(c) and (d)] streptavidin (STA) were injected separately under clean HEPES buffer solution to [(a) and (b)] reference sensors and [(c) and (d)] working sensors, respectively.

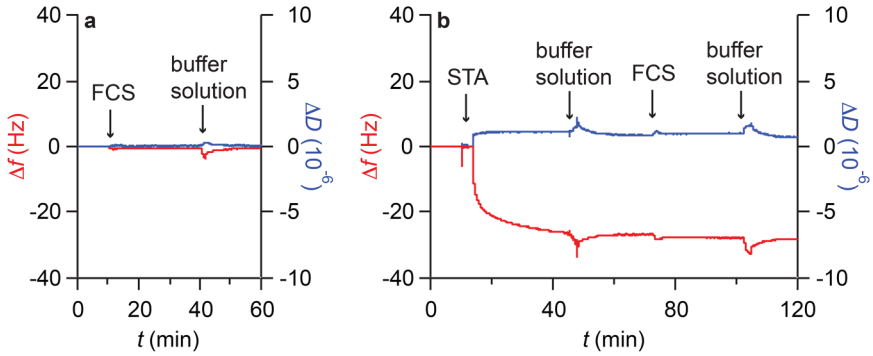

FIG. 5. QCM-D measurements, where 0.1% FCS dissolved in HEPES buffer solution was injected onto the working sensor (PLL-PEG-biotin) either (a) directly or (b) after the blocking of the electrode by streptavidin (25 μg/ml).

The opposite trend was observed when the control experiments were performed using QCM-D. The nonspecific binding was barely visible in QCM-D when FCS was injected directly [Fig. 5(a)] or after blocking the working sensor with streptavidin [Fig. 5(b)], and the specific binding of streptavidin presents a large frequency shift due to the adsorbed mass [Fig. 5(b)]. The fact that the nonspecific binding induced an impedance shift but did not change the adsorbed mass in QCM-D implies that the nonspecific binding in this case is probably the adsorption of ions, rather than proteins.

The STA-concentration dependence in the differential signals that we observed in Figs. 2 and 3 can be explained as a consequence of the coverage of the working electrodes by STA-biotin binding, which indirectly altered the signal by suppressing the accessibility of ions in FCS to the electrode. This interpretation is reasonable, because the response from the working sensor is greater at low STA concentrations [red in Figs. 2, 3(a), and 3(b) for 0.5-1 μg/ml], whereas it becomes smaller at higher STA concentrations [red in Figs. 2 and 3(c)–3(e) for 5-50 μg/ml], which is in agreement with the loss of FCS signal due to the coverage of the electrode by STA. This was also confirmed by a control experiment, where FCS was injected without STA in working and reference sensors, where their responses are very similar [Fig. S7 (Ref. 18)]. This is a phenomenon that takes place only in the presence of nonspecific binding, which is rarely even considered in the design of the impedance biosensing.

This outcome implies that impedance sensing in the presence of background molecules is a complex situation, because if the analyte alone does not induce significant impedance signals, as in the present case with streptavidin, the major differential signal (the difference between working and reference sensors) originates from the blocking of nonspecific binding. However, if the analyte alone induces a large impedance signal, the differential signal in the presence of background molecules will be a sum of the signal from the analyte and the one from blocking nonspecific binding. Depending on the properties of the analyte and the background molecules, these two signals can be either constructive (enhancing the signals) or distractive (canceling out the signals), thus the presence of nonspecific binding can increase or decrease the signal.

IV. CONCLUSION

We studied the effect of background molecules on the performance of differential impedance biosensing with PLL-g-PEG-biotin-coated gold electrodes for the detection of STA in the presence of 0.1% FCS. We were disappointed to find that our system can only detect the presence of STA above 5 μg/ml and that the exact STA concentration cannot be estimated because the differential signal immediately saturates at higher STA concentrations. The lowest STA concentration detected in the presence of 0.1% FCS in this work (5 μg/ml) is 1 order of magnitude higher (worse) than that from the previous avidin impedance-based biosensor in the absence of background proteins (≈100 ng/ml)[16] and 9 orders of magnitude higher than the best impedance biosensor reported in the literature (fg/ml).[4] This result highlights how the presence of background molecules changes the sensitivity of impedance biosensing by orders of magnitude. Interestingly, the origin of the differential signal was not due to the electrochemical properties of STA itself, but rather because the coverage of the electrode by STA indirectly modulated the electrical signal by suppressing the accessibility of FCS components to the electrode. The limit of detection in impedance biosensing depends greatly on the electrochemical properties of the analyte, the electrodes, and the amount and type of the background molecules; thus, the results shown in this work cannot be simply extrapolated for other types of impedance sensors. Nevertheless, this work implies that all of the impressive limits of detections reported in the literature will not be valid when those sensors are used with clinical samples with background molecules. In addition, we observed a phenomenon that takes place only in the presence of nonspecific binding. Such an effect must be investigated further, to design a device that works in realistic, diagnostic situations.

ACKNOWLEDGMENTS

The authors thank Alberto Morpurgo and Ignacio Gutierrez (University of Geneva) for granting access to and sharing their expertise with the electron-beam evaporator and Michal Borkovec (University of Geneva) for access to QCM-D.

[1](a) J. S. Daniels and N. Pourmand, Electroanalysis **19**, 1239 (2007); (b) V. M. Mirsky, M. Riepl, and O. S. Wolfbeis, Biosens. Bioelectron. **12**, 977 (1997).
[2]R. Richter, A. Mukhopadhyay, and A. Brisson, Biophys. J. **85**, 3035 (2003).
[3](a) T. Sannomiya, C. Hafner, and J. Voros, Nano Lett. **8**, 3450 (2008); (b) A. Dahlin, M. Zach, T. Rindzevicius, M. Kall, D. S. Sutherland, and F. Hook, J. Am. Chem. Soc. **127**, 5043 (2005).
[4]M. Dijksma, B. Kamp, J. C. Hoogvliet, and W. P. van Bennekom, Anal. Chem. **73**, 901 (2001).
[5]M. Sajid, A. N. Kawde, and M. Daud, J. Saudi Chem. Soc. **19**, 689 (2015).
[6](a) V. Gatterdam, A. Frutiger, K. P. Stengele, D. Heindl, T. Lubbers, J. Voros, and C. Fattinger, Nat. Nanotechnol. **12**, 1089 (2017); (b) C. Polonschii, S. David, S. Gaspar, M. Gheorghiu, M. Rosu-Hamzescu, and E. Gheorghiu, Anal. Chem. **86**, 8553 (2014).
[7](a) J. F. Masson, T. M. Battaglia, J. Cramer, S. Beaudoin, M. Sierks, and K. S. Booksh, Anal. Bioanal. Chem. **386**, 1951 (2006); (b) S. Choi and J. Chae, J. Micromech. Microeng. **20**, 075015 (2010); (c) G. L. Kenausis, J. Voros, D. L. Elbert, N. P. Huang, R. Hofer, L. Ruiz-Taylor, M. Textor, J. A. Hubbell, and N. D. Spencer, J. Phys. Chem. B **104**, 3298 (2000).
[8]P. J. Johnson, B. Portmann, and R. Williams, Br. Med. J. **2**, 661 (1978).
[9]P. Feng, C. Z. Huang, and Y. F. Li, Anal. Biochem. **308**, 83 (2002).
[10]H. X. Zhou, G. N. Rivas, and A. P. Minton, Annu. Rev. Biophys. **37**, 375 (2008).
[11](a) H. Maupas, A. P. Soldatkin, C. Martelet, N. JaffrezicRenault, and B. Mandrand, J. Electroanal. Chem. **421**, 165 (1997); (b) S. Ameur, H. Maupas, C. Martelet, N. Jaffrezic-Renault, H. Ben Ouada, S. Cosnier, and P. Labbe, Mat. Sci. Eng. C **5**, 111 (1997).
[12]S. Nizamov, V. Scherbahn, and V. M. Mirsky, Sens. Actuators B Chem. **207**, 740 (2015).
[13](a) O. A. Sadik, H. Xu, E. Gheorghiu, D. Andreescu, C. Balut, M. Gheorghiu, and D. Bratu, Anal. Chem. **74**, 3142 (2002); (b) X. Huang, W. H. Yeo, Y. H. Liu, and J. A. Rogers, Biointerphases **7**, 52 (2012).
[14]K. Sugihara, M. Delai, I. Szendro, O. Guillaume-Gentil, J. Vörös, and T. Zambelli, Sens. Actuators B **161**, 600 (2012).
[15]K. Jajcevic, M. Chami, and K. Sugihara, Small **12**, 4830 (2016).
[16]T. L. Lasseter, W. Cai, and R. J. Hamers, Analyst **129**, 3 (2004).
[17](a) F. Darain, D. S. Park, J. S. Park, and Y. B. Shim, Biosens. Bioelectron. **19**, 1245 (2004); (b) Y. Z. Fu, R. Yuan, L. Xu, Y. Q. Chai, Y. Liu, D. P. Tang, and Y. Zhang, J. Biochem. Biophys. Methods **62**, 163 (2005).
[18]See supplementary material at https://doi.org/10.1116/1.5082717 for the effect of the change in the offset voltages and the injection pressure on the impedance signals (Fig. S1); impedance spectra (Fig. S2); data from the real part (Z') and the absolute impedance ($|Z|$) (Figs. S3 and S4); impedance data at $f = 10\,000$ Hz (Fig. S5); a control experiment, where FCS was injected onto a working sensor (Fig. S6); and a control experiment, where 0.1% FCS was injected without STA into working and reference sensors (Fig. S7).